Macromolecular Research, Vol. 17, No. 11, pp 886-893 (2009)

Surface Characterization and Morphology in Ar-Plasma-Treated Polypropylene Blend

Jong-Il Weon and Kil-Yeong Choi*

Reliability Assessment Center of Chemical Materials, Korea Research Institute of Chemical Technology, Daejeon 305-600, Korea

Received March 24, 2009; Revised April 27, 2009; Accepted May 1, 2009

Abstract: Surface modifications using a radio frequency Ar-plasma treatment were performed on a polypropylene (PP) blend used for automotive bumper fascia. The surface characterization and morphology were examined. With increasing aging time, there was an increase in wettability, oxygen containing polar functional groups (i.e., C-O, C=O and O-C=O) due to oxidation, the amount of talc, and bearing depth and roughness on the PP surface, while there was a decrease in the number of hydrocarbon groups (i.e., C-C and C-H). AFM indicated that the Ar-plasma-treatment on a PP blend surface transforms the wholly annular surface into a locally dimpled surface, leading to an improvement in wettability. SEM showed that the PP layer observed in the non-plasma-treated sample was removed after the Ar-plasma treatment and the rubber particles were exposed to the surface. The observed surface characterization and morphologies are responsible for the improved wettability and interfacial adhesion between the PP blend substrate and bumper coating layers.

Keywords: plasma, surface characterization, polypropylene.

Introduction

The main advantage of polypropylene (PP) and polyolefins is their high performance-to-cost ratio. They have a variety of good properties such as light weight, thermal stability, chemical resistance and easy manufacturing. In spite of those merits, many industrial applications have still been limited due to their hydrophobic characteristics.[1-3]

Surface modifications of polypropylene and polyolefin polymers using plasma-based process have converted a desirable surface characterizations, i.e., from a hydrophobic surface to a hydrophilic one. The plasma processing helps to improve the surface properties such as the adhesion of coating, wettability, printability, and bio-compatibility.[4-13] In addition, no change of the bulk polymer property is observed since plasma treatment has an effect on only several molecular layers from polymer surface.[14-16] This type of plasma treatment relatively requires short exposure time at low power. Various gases and gas mixtures have been employed to a low pressure plasma process. Especially, inert gases (Ar, He) plasma treatment can be used to generate free radicals and cross-linking on polymer surface.[8,10,17] The electrical energy induced by plasma source dissociates the inert gas into electrons, ions, photons, meta-stable species and free radicals. The generated free radicals and electrons collide with the polymer surface and break down its covalent bonds. At this stage, in order to create thermodynamically stable functional groups on the polymer surface, the free radicals on the polymer surface may react to the O_2 and H_2O in the atmosphere.[14-16]

Recent development in plasma-based processes enables that polypropylene and other polyolefins are increasingly being applied to automotive industry through the modification of original surface characteristics.[18,19] Nowadays, automotive bumper fascia has been made of polypropylene blend. The bumper fascia is painted with various colors. For such an application, the surface modification *via* plasma processing takes an important role to improve the paint adhesion on PP matrix.

This study, which is part of a larger effort to improve the surface properties of PP blend for engineering applications, is to gain fundamental understanding on the surface characteristics of plasma-treated PP blend. It is expected that approaches for improving surface characterizations of PP blend used in automotive bumper fascia can be established. A number of technical approaches, such as contact angle measurement, scanning electron microscopy (SEM), X-ray photoelectron spectroscopy (XPS), Fourier transform-infrared spectroscopy (FTIR) and atomic force microscopy (AFM) were utilized to investigate the surface morphology of plasma-treated PP blend. The dependency of plasma aging time is examined. The underlying mecha-

*Corresponding Author. E-mail: kychoi@krict.re.kr

nisms of the increase in wettability for plasma-treated PP blend are also discussed.

Experimental

Materials and Sample Preparation. Polypropylene copolymer (Hyundai EP Co., Ltd.), which has a melt index of 11 g/10 min and a density of 0.99 g/cc, was used in this study. The PP resin was compounded with talc of 12 wt% and ethylene-propylene-diene monomer (EPDM) rubber of 25 wt%. Injection-molded 3-mm-thick PP blend sheets with 98 mm wide by 345 mm long were prepared. The PP blend sheets were cut a size of 110×25×3 mm for plasma treatment and then were clean with distilled water and ethyl alcohol. After cleaning all samples were immediately sealed in a polyethylene bag and kept in a vacuum desiccator.

Plasma Treatment. For surface modification of PP blend, it was to expose the surfaces to a high-energy atmospheric pressure (0.5 Mbar) plasma, using a Polaron PT7160 plasma etcher. All samples were treated with Ar gas plasma with 100 W radio frequency (RF) power at a constant gas flow rate of 5 cm^3/min for 60, 180 and 300 s.

Surface Characterization. The contact angle (SEO 300, Surface & Electro-Optics Corp., Korea) and the wettability of plasma-treated PP blends were directly measured on each of five drops placed on the surface. The volume of a drop placed with micro-syringe was 3 mm^3.

X-ray photoelectron spectroscopy (XPS) observations were conducted on Shimadzu Axis NOVA, with an Al K_α (1486.6 eV) monochromatic x-ray source operating at 150 W, with 20 mA current and 15 kV voltage. The pressure in the sample chamber is 10^8 torr. Survey scans were collected in the range of 0-1,500 eV binding energy with a resolution of 1.0 eV and a pass energy of 160 eV. High resolution scans were taken on the C 1s and O 1s with the energy resolution of 0.1 eV and a pass energy of 20 eV.

FTIR spectroscopy was used to investigate the chemical variation due to plasma treatment. Attenuated total reflection (ATR) spectra were recorded on Nicolet Magna IR 560 with germanium crystal.

Atomic force microscopy (AFM) was used to measure the surface roughness and the bearing depth of non-plasma-treated and plasma-treated PP blends. AFM images were taken using a multimode Nanoscope IV (Digital Instrument, Santa Barbara, CA) in tapping mode. The survey area was 10×10 μm.

Field emission scanning electron microscopy (FE-SEM) observations were carried out on JEOL JSM 6700F operated at an accelerating voltage of 10 kV. In addition, a preferential etching of EPDM phase was performed in cyclohexane solution for 15 min to observe the change of surface morphology due to Ar-plasma treatment. The samples were cryogenically fractured in liquid nitrogen prior to etching. Then the fractured and etched samples were observed with above SEM instrument. In order to investigate the change of atomic components before and after doing plasma treatment, energy dispersive spectroscopy (EDS) analyses were conducted on Thermo NORAN operating with an accelerating voltage of 20 kV.

Results and Discussion

Wettability. Figure 1 shows typical photographs of contact angles and wettabilities on the surfaces of non-plasma-treated and plasma-treated PP blends as a function of ageing time. An increase in aging time leads to decrease the contact angle of plasma-treated PP blends, as summarized in Table I, while the wettability would be improved. These results illustrate the plasma-induced hydrophilic effect on the PP blend surfaces. Interestingly, an abrupt decrease in contact angle is observed on the surface of plasma-treated PP blend for 60 s, compared to the neat PP blend received no plasma treatment. This means that the Ar-plasma treatment is a useful method for tailoring the wettability, hydrophilicity and interfacial adhesion of PP blend surface with originally low surface free energy, through surface modification.

SEM and EDS Observation. Figure 2 shows the SEM micrographs indicating the different surface morphology of

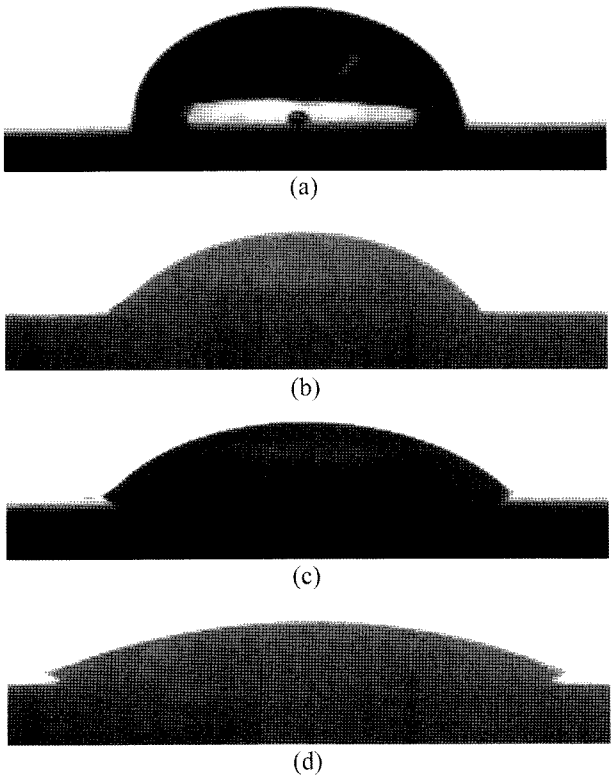

Figure 1. Typical photographs of contact angle for the differently Ar-plasma treated PP blends: (a) neat PP blend (94.1°), (b) PP blend/Ar/60 s (56.6°), (c) PP blend/Ar/180 s (42.6°), and (d) PP blend/Ar/300 s (27.5°).

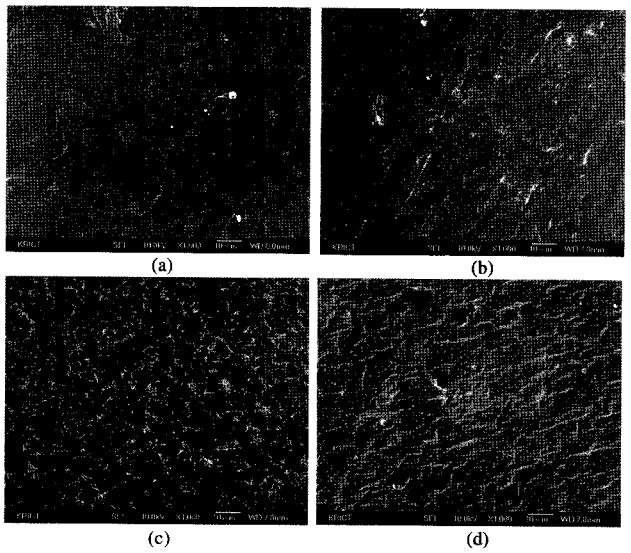

Figure 2. SEM micrographs of the differently Ar-plasma treated PP blend surfaces: (a) neat PP blend, (b) PP blend/Ar/60 s, (c) PP blend/Ar/180 s and (d) PP blend/Ar/300 s.

neat and plasma-treated PP blends with respect of the aging time. As shown in Figure 2, the surface roughness seems to depend on aging time. A longer plasma aging time appears to cause an increase in roughness. However, a significant variation in roughness among these SEM micrographs is clearly not observed by the naked eye owing to the depth scale in roughness. AFM work is further employed to confirm and quantify the aforementioned. The EDS result reveals that chemical composition of neat PP blend consist of C of 82.97 wt%, O of 12.35 wt%, Mg of 2.07 wt% and Si of 2.61 wt%; C and O atom arises from PP and EPDM rubber, and Mg and Si atom comes from talc particles. As treating the PP blend surface with Ar-plasma, no significant difference in atomic wt% concentration is observed. The concentration of O, Si and Mg atoms slightly increases with increasing aging time. This may imply that new function groups with O atom are created and the talc particles are exposed on the surface of plasma-treated PP blends. A detailed description regarding above conjecture will be addressed when XPS results are presented.

AFM Observation. The AFM study was employed to investigate the detailed topography in PP blends. The bearing depth, which is presented by average height in bearing area, and roughness, which is expressed by root mean square (RMS) value, of neat and plasma-treated PP blends with respect of the aging time are summarized in Table I. The surface of neat PP blend has a set value of bearing depth and roughness; (206.3 nm, 43.6 nm), while those of Ar-plasma-treated samples for 60 s, 180 s, and 300 s have a set values of (274.0 nm, 78.0 nm), (345.3 nm, 100.7 nm) and (456.2 nm, 107.0 nm), respectively. The longer aging time enables the rougher and more highly etched surface of PP blends.[20] As

Table I. The Results of Contact Angle Measurement and AFM Analysis for the Differently Ar-Plasma Treated PP Blends

Sample	Contact Angle (degree)	RMS Roughness (nm)	Bearing Depth (nm)
Neat PP blend	94.1±5.2	43.6	206.3
PP blend/Ar/60 s	56.6±4.6	78.0	274.0
PP blend/Ar/180 s	42.6±3.7	100.7	345.3
PP blend/Ar/300 s	27.5±3.8	107.0	456.2

shown in Figure 3(a), the annular morphology can be observed on the surface of neat PP blend. However, as treating Ar-plasma, those morphologies are gradually disappeared. Instead, the locally dimpled areas are observed (Figure 3(b-d)) but the surface morphology is still uniform overall. This can be explained by the physical etching effect of Ar-plasma. The Ar-plasma treatment provides a relatively uniform etching on the whole surface since Ar is a single inert gas.[8] It should be mentioned that there is a good correlation between the AFM result and the contact angle result with respect to the plasma aging time, indicating that the improved wettability can be explained by the increase in bearing depth and roughness of Ar-plasma treated surfaces.

XPS Analysis. The chemical composition and the binding energy of neat and plasma-treated PP blends at different aging times were observed. Detectable changes on the elemental surface composition of plasma-treated samples can be shown in Figure 4. The survey spectra of the differently treated samples reveal that the binding energies of 285 and 533 eV are associated with the C 1s and O 1s, respectively. A proportional increase in oxygen and silicon concentration is observed as the aging time is prolonged, while a progressive decrease in hydrocarbon concentration occurs (Table II). This implies that the Ar-plasma treatment has an effect on increasing oxygen-containing polar functional groups on the PP blend surface. In general, two reaction mechanisms during Ar-plasma treatments are involved. One is the functionalization reaction as a result of inelastic collisions between the substrate and the activated ion species including electrons and free radicals. The other is the chemical etching reaction to form volatile gaseous products by cutting off molecular chains as active oxygen species are implanted into the surface atoms. In the case of Ar-plasma treatment, the effect of functionalization reaction is predominant compared to that of chemical etching reaction since no chemical etching reaction between the surface atoms and the activated Ar species occurs theoretically. Here, an increase in oxygen-containing polar functional groups shown in Ar-plasma treated samples can be explained by the fact that the free radicals created on the surface during Ar-plasma treatment may readily react with the oxygen and moisture when samples are placed in an experimental atmosphere for plasma treatment.[21-24] Finally, two reaction

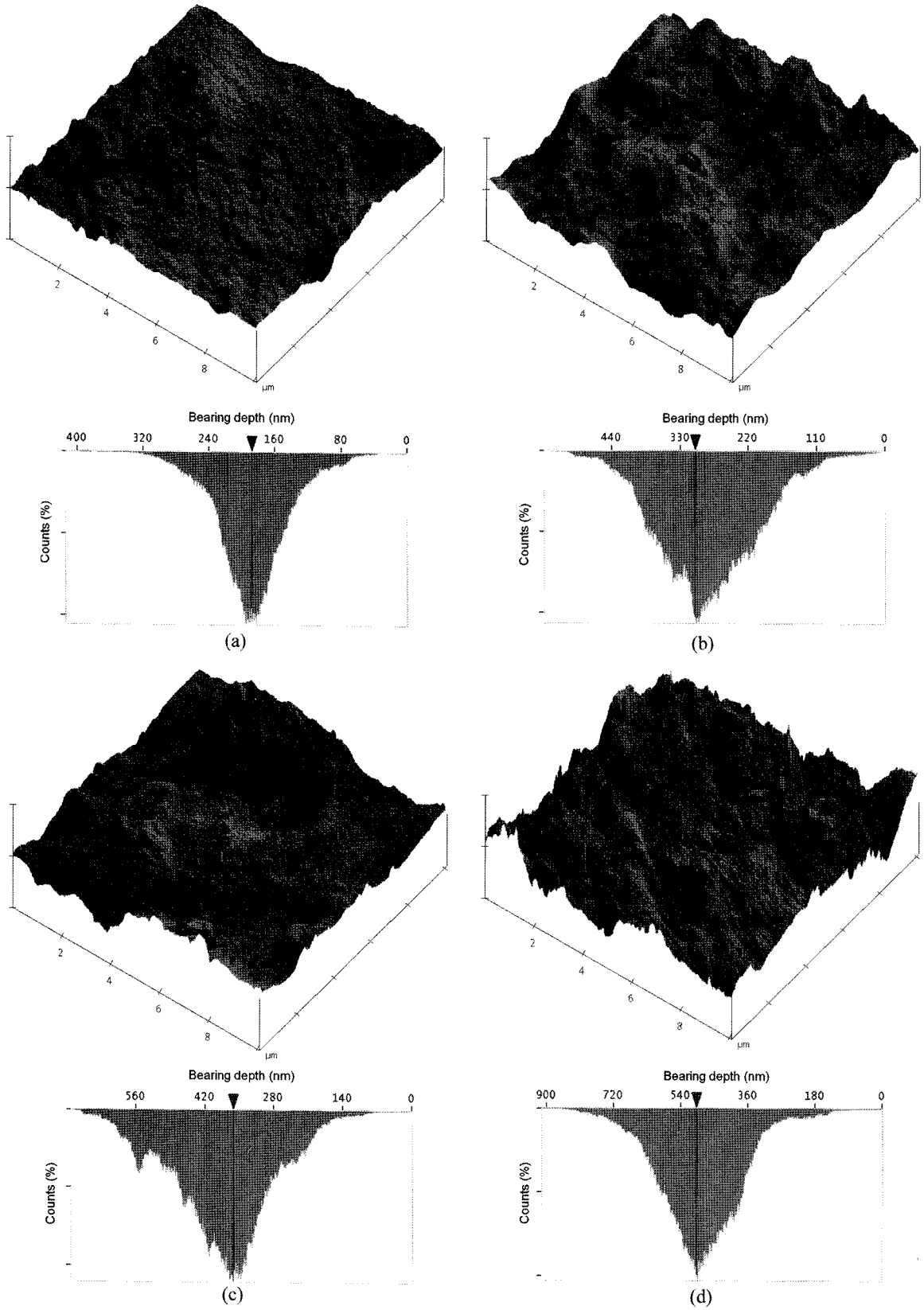

Figure 3. Three dimensional AFM images showing RMS roughness and bearing depth for the differently Ar-plasma treated PP blend surfaces: (a) neat PP blend (43.6, 206.6 nm), (b) PP blend/Ar/60 s (78.0, 274.0 nm), (c) PP blend/Ar/180 s (100.7, 345.3 nm) and (d) PP blend/Ar/300 s (107.0, 456.2 nm).

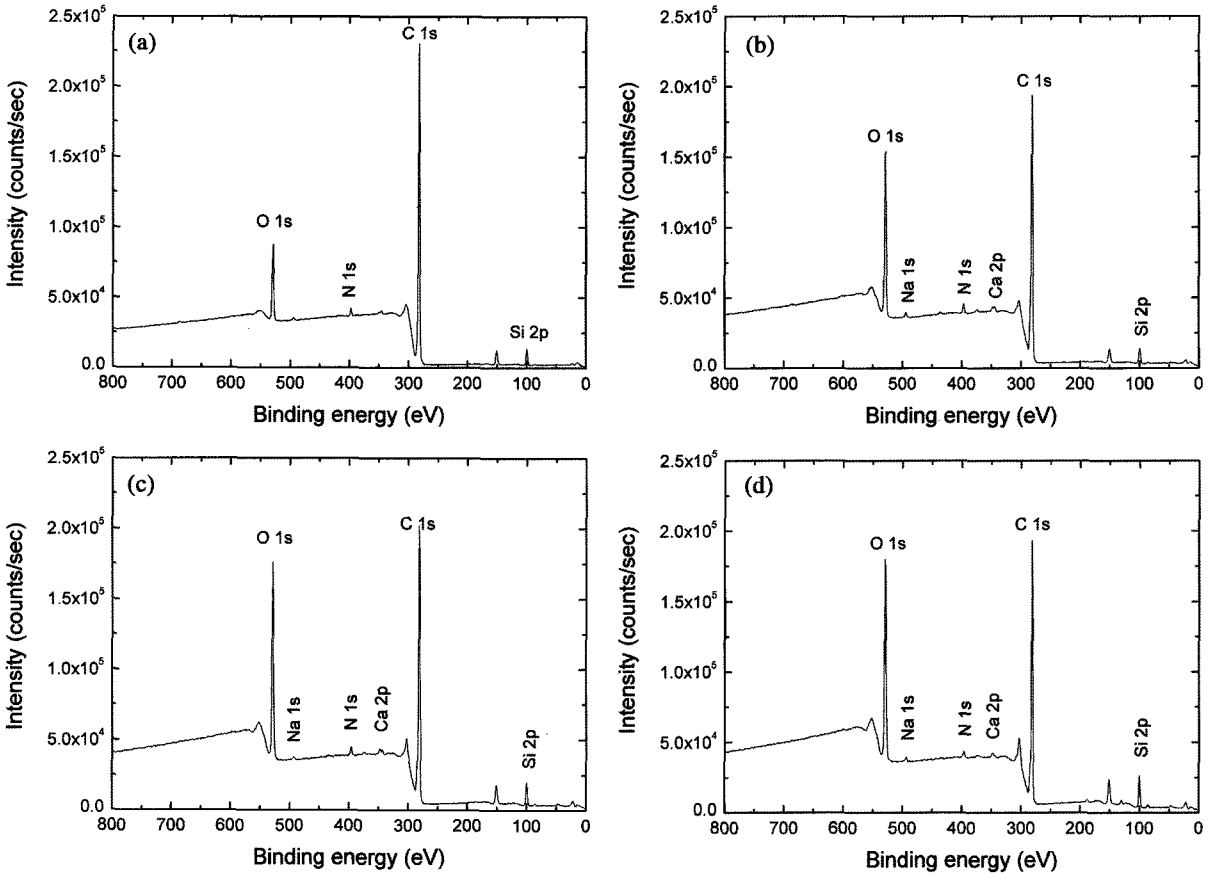

Figure 4. XPS survey spectra of the differently Ar-plasma treated PP blend surfaces: (a) neat PP blend, (b) PP blend/Ar/60 s, (c) PP blend/Ar/180 s and (d) PP blend/Ar/300 s.

Table II. Atomic Percent Concentration and Atomic Ratio of the Differently Ar-Plasma Treated PP Blends

Sample	Atomic Concentration (%)						Atomic Ratio (%)	
	C 1s	O 1s	Si 2p	N 1s	Ca 2p	Na 1s	O/C	Si/C
Neat PP blend	86.15	8.81	3.76	1.27	<0.1	<0.1	10.23	4.36
PP blend/Ar/60 s	76.65	16.80	3.88	1.91	0.57	0.19	21.92	5.06
PP blend/Ar/180 s	72.57	19.80	5.12	1.79	0.56	0.16	27.28	7.06
PP blend/Ar/300 s	67.79	22.05	7.38	1.96	0.57	0.25	32.53	10.89

mechanisms during Ar-plasma treatments may progress simultaneously. In addition, the Si 2p peak which arises from talc particles of PP blend increases with increasing aging time. This can be related to the physical sputtering effect. During Ar-plasma treatment, the talc particles existed outward PP matrix will be exposed onto the surface by etching reaction. Moreover, negligible peaks of N 1s, Ca 2p and Na 1s are observed.

High resolution scans of the C 1s peak of the differently treated PP blends are performed to find out detailed reaction mechanisms (Figure 5). High resolution C 1s peak of neat PP blend consists of a major peak centered at 285.0 eV.[8,10,25] As the C 1s peak is deconvoluted, three Gaussian components (i.e., functional groups) such as C_I (C-C/C-H), C_{II} (C-O) and C_{III} (C=O) are curve-fitted. Interestingly, samples after Ar-plasma treatment present new functional group such as C_{IV} (O-C=O) corresponds to the binding energy of 289.1 eV. The appearance of C_{IV} might be related to the esterification of OH group generated during plasma treatment.[26,27] The amount of C_{II}, C_{III} and C_{IV} group increases with increasing aging time, while the amount of C_I decreases (Table III). These increases in C_{II}, C_{III} and C_{IV} groups suggest that the hydrocarbon chains, i.e., carbon-carbon and carbon-hydrogen, have partially been oxidized. Progressive removal of hydrocarbon groups and formation of carboxyl group due to hydrocarbon chain oxidation result in the creation of

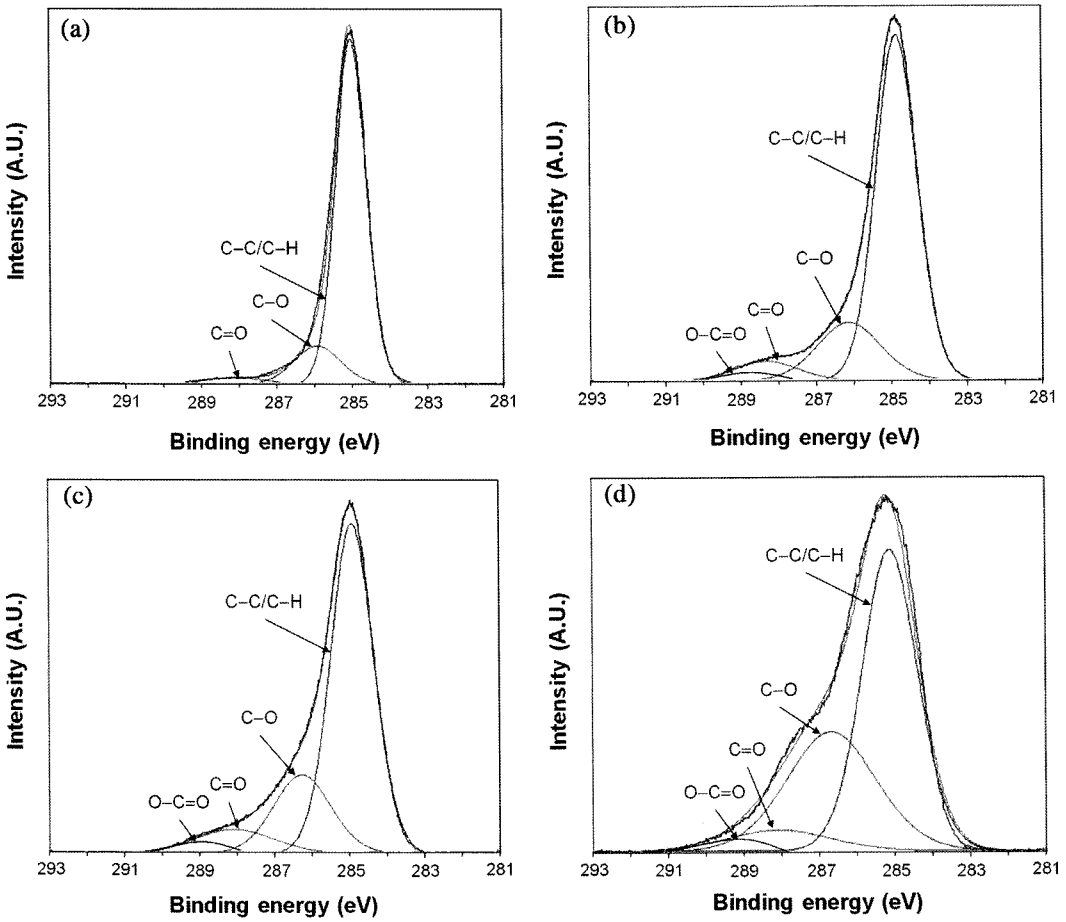

Figure 5. Deconvoluted high resolution XPS C 1s spectra of the differently Ar-plasma treated PP blend surfaces: (a) neat PP blend, (b) PP blend/Ar/60 s, (c) PP blend/Ar/180 s and (d) PP blend/Ar/300 s.

Table III. Relative Intensity of the Deconvoluted C 1s Spectra of the Differently Ar-Plasma Treated PP Blends

Sample	C-C/C-H	C-O	C=O	O-C=O
Neat PP blend	82.10	14.30	3.60	-
PP blend/Ar/60 s	73.10	19.10	6.60	1.20
PP blend/Ar/180 s	68.00	21.80	8.60	1.60
PP blend/Ar/300 s	56.25	35.02	9.17	2.56

oxygen containing functional groups and the transformation into hydrophilic state.

FTIR Analysis. FTIR analysis was conducted to compare to the XPS results. Figure 6 displays the FTIR spectra of neat PP blend and plasma-treated PP blends with respect of the aging time. The transmittance band arising around 1710 cm^{-1} corresponds to C=O bond originated from carboxyl group. The broad peak at 3200-3400 cm^{-1} is assigned to O-H derived from hydroxyl group. A set of progressive increases in intensities of these bands are observed as the aging time increase. This result suggests that the hydrocarbon groups (C-C, C-H) locally undergo the oxidation on the PP blend surface owing to Ar-plasma treatment. It should be mentioned that the results shown in FTIR analysis are in good agreement with the XPS results.

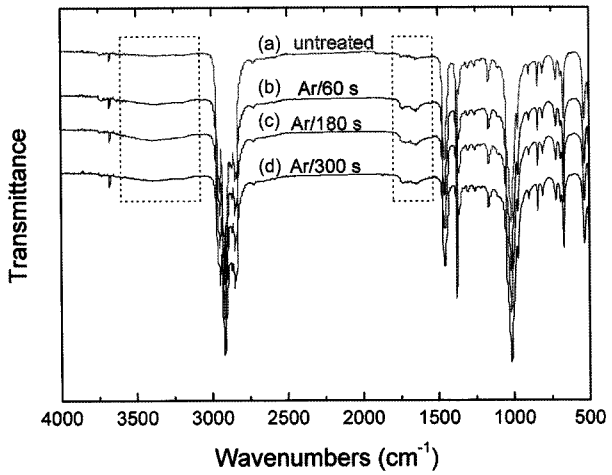

Figure 6. ATR-FTIR spectra of the differently Ar-plasma treated PP blend surfaces: (a) neat PP blend, (b) PP blend/Ar/60 s, (c) PP blend/Ar/180 s and (d) PP blend/Ar/300 s

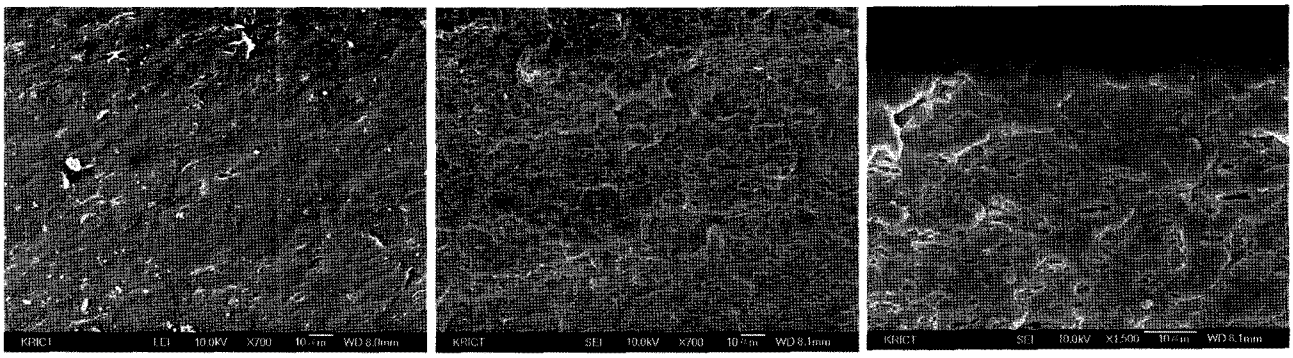

(a) (b) (c)

Figure 7. SEM micrographs of the etched neat PP blend sample taken from: (a) the surface area, (b) the middle of cross section area and (c) the margin of cross section area.

Morphology Observation. Figure 7 shows the surface morphologies of neat PP blend after etching with cyclohexane for 15 min. The SEM micrograph on surface area of neat PP is shown in Figure 7(a). Compared with the SEM micrograph of non-etched neat PP blend sample (Figure 2(a)), no variation of morphology is found. Etched EPDM phases can rarely be found on the surface, indicating that the EPDM rubber particles are almost not existed on the sample surface. Furthermore, many talc particles are still buried in PP matrix. However, well-dispersed EPDM rubber particles are observed in the cross section area (Figure 7(b)). EPDM phase was etched preferentially and could be clearly observed via SEM micrograph. The EPDM particles are removed by cyclohexane solution, leaving semi-spherical shape on the PP blend surface. Figure 7(c) shows the morphology of interfacial area between surface and cross section areas. Careful observation suggests that the PP layer (<150 μm) is observed toward the surface. This implies that the EPDM rubber particles do not exist in the PP layer. This phenomenon may be due to the big difference of melt index and/or viscosity between PP resin and EDPM rubber during injection molding process. It can be difficult for EPDM rubber with lower melt index to reach within 150 micrometer of the edge of injection-molded sample, compared to PP resin with higher melt index and/or lower viscosity.

In the other hand, the surface morphology of Ar-plasma treated PP blend for 300 s is shown in Figure 8. Interestingly, after Ar-plasma treatment, preferentially etched rubber sites are clearly observed on the surface area (Figure 8(a)), which could not be seen on the surface of Ar-plasma treated and non-etched PP blend (Figure 2(d)). In addition, many talc particles are exposed from PP matrix after Ar-plasma treatment. This finding can definitely address the reason that the Si 2p peak in XPS spectra increased with increasing aging time. Figure 8(b-c) present the SEM micrographs observed in the cross section area of Ar-plasma treated PP blend for 300 s. It should be pointed out that the PP layer shown above is removed out after Ar-plasma treatment. This phenomenon may promote the improvement of interfacial adhesion between PP blend surface and coating materials for automotive bumper fascia, since the EPDM rubber has higher wettability than PP resin. In other words, the exposed rubber plays an effective role in tethering the coating materials as an anchor. For automotive bumper fascia, the coating work consists of primer coating, base coating and clear coating progressively toward the surface of PP blends. In general, the primer has a good compatibility with both PP matrix and rubber particle. Therefore, the Ar-plasma treatment

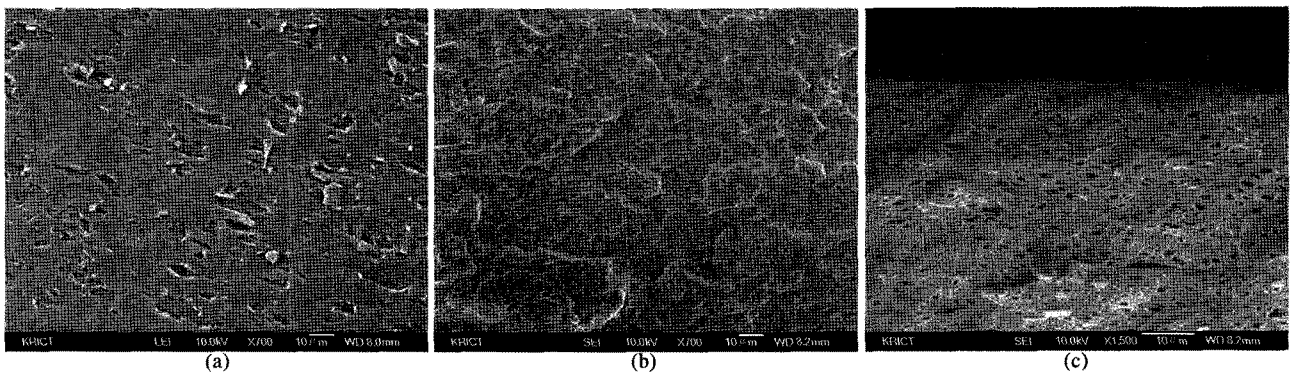

(a) (b) (c)

Figure 8. SEM micrographs of the Ar-plasma treated for 300 s and etched PP blend sample taken from: (a) the surface area, (b) the middle of cross section area and (c) the margin of cross section area.

on the PP blend surface is effective in giving the hydrophilic state, as well as in providing the anchoring effect for interfacial adhesion.

Conclusions

With an effort to improve the surface properties of polypropylene (PP) blend for engineering applications, the surface characteristics of Ar-plasma-treated PP blend are examined as a function of aging time. The changes in wettability of Ar-plasma treated samples are in proportion to the aging time. Observation by X-ray photoelectron spectroscopy shows that a significant increase in the ratio of oxygen to carbon due to functionalization reactions and a slight increase in the ratio of silicon to carbon owing to etching reaction. Moreover, the deconvolution of the C 1s photoelectron peak reveals an obvious surface modification of functional group nature. SEM observations show clearly the variation of surface morphology after Ar-plasma treatment. The PP layer shown in untreated sample is removed and the rubber particles are exposed on the surface, which may lead to improve the interfacial adhesion. For automotive industry, a simple and crucial core technique has been demanded in order to improve the wettability and interfacial adhesion of PP bumper fascia. Ar-plasma treatment could be nominated as one of reliable methodologies in providing the PP substrates with high wettability and interfacial adhesion performance.

References

(1) R. G. Raj, B. V. Kokta, D. Maldas, and C. Daneault, *J. Appl. Polym. Sci.*, **37**, 1089 (1989).
(2) J. I. Weon, K. T. Gam, W. J. Boo, H. J. Sue, and C. M. Chan, *J. Appl. Polym. Sci.*, **99**, 3070 (2006).
(3) J. I. Weon and H. J. Sue, *J. Mater. Sci.*, **41**, 2291 (2006).
(4) T. W. Kim, J. H. Lee, J. W. Back, W. G. Jung, and J. Y. Kim, *Macromol. Res.*, **17**, 31 (2009).
(5) C. M. Chan, in *Polymer Surface Modification and Characterization*, H. Gardner, Ed., Hanser Verlag, Munich, 1994.
(6) E. D. Seo, *Macromol. Res.*, **12**, 608 (2004).
(7) E. D. Seo, *Macromol. Res*, **12**, 134 (2004).
(8) O. J. Kwon, S. W. Myung, C. S. Lee, and H. S. Choi, *J. Colloid Interf. Sci.*, **295**, 409 (2006).
(9) O. J. Kwon, S. Tang, S. W. Myung, N. Lu, and H. S. Choi, *Surf. Coat. Technol.*, **192**, 1 (2005).
(10) K. E. Ryu, H. Rhim, C. W. Park, H. J. Chun, S. H. Hong, J. J. Kim, and Y. M. Lee, *Macromol. Res.*, **35**, 451 (2003).
(11) R. Molina, P. Jovancic, D. Jocic, E. Bertran, and P. Erra, *Surf. Interf. Aanl.*, **35**, 128 (2003).
(12) H. Park, K. Y. Lee, S. J. Lee, K. E. Park, and W. H. Park, *Macromol. Res.*, **15**, 238 (2007).
(13) M. Zeniewicz, *J. Adhes. Sci. Technol.*, **15**, 1769 (2001).
(14) F. Caiazzo, P. Canonico, R. Nigro, and V. Tagliaferri, *J. Mater. Process. Technol.*, **58**, 96 (1996).
(15) S. L. Kaplan and P. W. Rose, *Plast. Eng.*, **34**, 1542 (1988).
(16) S. L. Kaplan and P. W. Rose, *Plast. Eng.*, **44**, 77 (1988).
(17) K. Tanaka, T. Inomata, and M. Kogoma, *Thin Solid Films*, **386**, 217 (2001).
(18) C. K. Jung, I. S. Bae, S. B. Lee, J. H. Cho, E. S. Shin, S. C. Choi, and J. H. Boo, *Thin Solid Films*, **506-507**, 316 (2006).
(19) L. Carrino, W. Polini, and L. Sorrentino, *J. Mater. Process. Technol.*, **153-154**, 519 (2004).
(20) M. C. Coen, G. Dietler, S. Kasas, and P. Gröning, *Appl. Surf. Sci.*, **103**, 27 (1996).
(21) F. Denes, L. D. Nielsen, and R. A. Young, *Lignocellulosic-Plastic Compos.*, **1**, 61 (1997).
(22) J. R. Chen, *J. Appl. Polym. Sci.*, **62**, 1325 (1996).
(23) H. S. Sabharwal, F. Denes, L. Nielsen, and R. A. Young, *J. Agric. Food. Chem.*, **41**, 2202 (1993).
(24) T. Wakida, K. Takeda, I. Tanaka, and T. Takagishi, *Text. Res. J.*, **59**, 49 (1989).
(25) N. V. Bhat, D. J. Upadhyay, R. R. Deshmukh, and S. K. Gupta, *J. Phys. Chem. B*, **107**, 4550 (2003).
(26) Z. Q. Hua, *Plasma induced surface modification of lignocellulosic and synthetic polymers*, PhD Thesis, University of Wisconsin-Madison, 1996.
(27) R. A. Young, F. Denes, Z. Q. Hua, and R. Sitaru, *Proceedings of 9th International Symposium on Wood and Pulping Chemistry*, 1997, pp 1291.